Model Predictive Control for Closed-Loop Deep Brain Stimulation

Sebastian Steffen* Mark Cannon* Huiling Tan† Jean Debarros†

***Abstract*— This paper describes a model predictive control (MPC) algorithm for Deep Brain Stimulation (DBS) implants that are used to treat common movement disorders. DBS is currently used in clinical practice in open-loop with constant stimulation, which shortens the effective lifespan of the treatment and can lead to unpleasant side-effects. The goal of closed-loop control is to alleviate symptoms with minimal stimulation. The controller is based on a model of the amplitude of beta-band (13-30 Hz) oscillations of population-level neural activity at the site of the implant, which is a bio-marker related to the presence of symptoms of Parkinson's Disease. We present a two-stage approach in which a dynamic model for bio-marker activity is identified from data after applying a linearizing transformation, followed by a regulation stage using the identified model together with a model of response to stimulation based on average patient data. A Kalman filter is used to estimate the state of both the stimulation response and the nominal beta activity. The controller is compared to thresholded on/off (bang-bang) and proportional-integral (PI) feedback controllers, which are the most advanced form of control tested *in vivo* to date. Simulations demonstrate reductions in control input for similar levels of tracking error.**

***Keywords*— neuromodulation, model predictive control, state estimation, system identification**

I. Introduction

Deep Brain Stimulation (DBS) is a neuromodulation technique used to treat Parkinson's Disease (PD) and other motion and affective disorders such as essential tremor and dystonia [1]. The treatment involves surgically implanting electric leads in deep brain structures (e.g. the subthalamic nucleus for PD), and locally stimulating groups of neurons with pulses of electric activity. Conventionally, DBS is delivered using a constant stimulation pattern with fixed amplitude, frequency, and pulse width, which leads to stimulation being active even during periods of healthy brain activity [2]. This results in a faster decline in efficacy of the treatment due to habituation to the stimulation, and more extensive side-effects than what could be achieved with targeted stimulation [3].

Increased amplitude in so-called beta-band (13-30Hz) oscillations of Local Field Potentials (LFP) recorded at the site of the implant are a regular feature of PD, and suppression of this activity is associated with improvement of motor symptoms [4], [5]. This motivates the use of beta activity measured as a feedback signal for closed loop control of DBS [3]. The goal of the controller is to regulate activity to the baseline level while minimizing applied stimulation. Until now, only simple algorithms such as bang-bang (i.e. on/off) control, and proportional or dual-threshold control algorithms based on beta activity feedback have been tested in Parkinsonian patients (see e.g. [6], [7], [8]).

A wider range of control algorithms have been investigated in simulation-based studies. Some approaches employ different control objectives, such as only suppressing bursts of beta-band activity that exceed a certain duration [9]. Other approaches use additional control signals such as patient muscle activity together with a bank of PI controllers tuned for various operating points [10]. Several studies have proposed optimal predictive control schemes; some use nonlinear models [11], while others identify linear models (e.g. ARX or using subspace methods) of beta-band activity suppression online [12], [13]. However, to the best of the authors' knowledge, none of the predictive control schemes aim to model the dynamics of nominal bio-marker activity, (e.g. beta-band bursting activity in PD), and only model the response to stimulation.

We use a model of the LFP response to stimulation derived from averaged patient data [14] to develop a strategy for model predictive control (MPC) with online state estimation. We propose a two-stage approach, first applying a linearizing transformation and identifying a linear model of the beta activity, and then employing this model in a regulation phase, using MPC to suppress bursting activity. Crucially, this approach anticipates short-term variations in beta activity, allowing more effective control interventions than existing DBS strategies. It also optimizes the balance of regulation and stimulation effort while keeping stimulation parameters within safe limits. With this approach, the controller can adapt to the nominal activity of specific patients, and the procedure can be reinitialized to adapt to disease progression or different patient states, such as waking or sleeping.

The remainder of this paper is structured as follows: Section II describes the model of the beta biomarker and the control objective, Section III describes the design of an MPC strategy for the Closed Loop DBS system, Section IV presents a numerical comparison of the proposed controller against a PID controller and a bang-bang controller.

II. Problem Formulation

As a basis for controller design and testing via simulations, we make use of the model of LFP beta oscillation response described in [14]. The important features of this model are summarized in Sections II-A and II-B.

*Department of Engineering Science, University of Oxford, OX1 3PJ, UK. {sebastian.steffen,mark.cannon}@eng.ox.ac.uk

†MRC Brain Network Dynamics Unit, Nuffield Department of Clinical Neurosciences, University of Oxford, OX1 3TH, UK. {huiling.tan, jean.debarros}@ndcn.ox.ac.uk

A. Beta-Oscillation Envelope Model

The envelope of the beta-band activity in the subthalamic nucleus at time t is denoted $z(t) \in \mathbb{R}^+$. This envelope is related to the nominal activity, $z_\beta(t)$, the DBS attenuation effect $\eta(t)$ and bounded, zero-mean independent and identically distributed (i.i.d.) measurement noise $\zeta(t)$ as follows [14]

$$z(t) = z_\beta(t) \cdot e^{-\eta(t)} + \zeta(t). \tag{1}$$

The stimulation effect $\eta(t)$ is governed by a dynamical system which has the instantaneous power of electrical stimulation at time t as its input.

B. Stimulation Effect

The stimulation response is modelled as the output of a second order continuous-time system,

$$\begin{aligned} \dot{x}_c(t) &= \begin{bmatrix} -1/\tau_1 & 0 \\ k/\tau_2 & -1/\tau_2 \end{bmatrix} x_c(t) + \begin{bmatrix} k/\tau_1 \\ 0 \end{bmatrix} u(t) \\ \eta(t) &= \begin{bmatrix} 0 & 1 \end{bmatrix} x_c(t), \end{aligned} \tag{2}$$

where the control input $u(t)$ represents the voltage applied to the stimulator, which is constrained to lie in the range $u \in [0, u_{\max}]$. The nominal values of the stimulation response parameters in the model (2) are given by

$$k = 62.11, \quad \tau_1 = 0.05, \quad \tau_2 = 0.25.$$

These constants are derived based on averaged data from multiple patients [14]. In practice these values will differ across patients, and will also vary across as a result of disease progression, and of shorter time-scale fluctuations.

C. Control Objective

The goal of CLDBS is to suppress bursts of Parkinsonian activity with the minimum possible control input. Typically bursts exceeding 200ms in duration are correlated with motor symptoms. Some existing methods for attempting to predict the onset [15] and duration [16] of bursts rely on neural networks which require significant computational resources. These methods will not be considered in this work, since the processing power on DBS hardware is low, and there are significant constraints on energy usage due to the fact that the power supply is provided by batteries implanted in the patient [17]. Therefore, the goal of the controller will be to suppress beta activity which exceeds the baseline level z_0. This suggests a quadratic cost index for the optimal control law defined over a horizon T of the form

$$\int_0^T \left(\phi([z(t) - z_0]_{\geq 0}) + Ru(t)^2 \right) dt \tag{3}$$

$$[z(t) - z_0]_{\geq 0} = \begin{cases} z(t) - z_0, & \text{if } z(t) \geq z_0 \\ 0, & \text{otherwise} \end{cases} \tag{4}$$

where $\phi : \mathbb{R}_{\geq 0} \to \mathbb{R}_{\geq 0}$ is a monotonically increasing function, and R is a positive control weighting.

III. Control Design

A. Linearization

We reformulate the model in (1) so that the effect of beta bursts appears as an additive disturbance in the stimulation response system. This can be done by defining a new measurement variable $y(t) = \ln(z(t))$. When the measurement noise component of the beta envelope is small, the effect of $\zeta(t)$ on $y(t)$ can be modelled (to first-order approximation) as an additive noise term v, which is i.i.d. and zero mean, but with a different magnitude than ζ,

$$y(t) = \beta(t) - \eta(t) + v(t), \tag{5}$$

where $\beta = \ln(z_\beta)$ and $\beta_0 = \ln z_0$. This formulation allows the use of MPC with a linear model and additive disturbance compensation. In discrete-time, the stimulation effect model (2) with a zero-order hold at the input is

$$\begin{aligned} x_{\eta,k+1} &= A_\eta x_{\eta,k} + B_\eta u_k \\ \eta_k &= \begin{bmatrix} 0 & 1 \end{bmatrix} x_{\eta,k} \end{aligned} \tag{6}$$

where $k = 0, 1, \ldots$ is the discrete time index.

B. Linear Model of Nominal Beta Activity

We propose a linear, autoregressive integrated (ARI) model for the dynamics of the beta-band activity bursts. This model expresses the change in the activity $\Delta\beta_k = \beta_k - \beta_{k-1}$ as a finite weighted sum of n_β past values:

$$\Delta\beta_k = \sum_{i=1}^{n_\beta} \alpha_i \cdot \Delta\beta_{k-i} + \delta_k \tag{7}$$

where δ_k is a bounded, stochastic, i.i.d. disturbance.

C. Nominal Beta Activity Model Parameter Identification

The effects of the nominal activity β and the stimulation effect η can be temporarily separated by holding the control input $u_k = 0$ over some identification window $k = 0, 1, \ldots, N_\beta$, thereby ensuring $\eta_k = 0$ for $k = 0, 1, \ldots, N_\beta$. This allows allows an estimate of the parameter vector

$$\theta_\beta = \begin{bmatrix} \alpha_1 & \alpha_2 & \cdots & \alpha_{n_\beta} \end{bmatrix}^\top$$

to be computed for the model in (7) using a least squares ARI identification approach.

D. Augmented model

The models of the stimulation effect (6) and beta activity bursts (7) can be combined into a single model for use within

a predictive control strategy:

$$\begin{aligned}
\chi_{k+1} &= A(\theta_\beta)\chi_k + Bu_k + w_k \\
y_k &= \begin{bmatrix} C_\eta & C_\beta \end{bmatrix} \chi_k \\
A(\theta_\beta) &= \begin{bmatrix} A_\eta & & \mathbf{0}^{2\times n_\beta} \\ & \begin{bmatrix} 1 & \alpha_1 & \alpha_2 & \dots & \alpha_{n_\beta} \\ 0 & \alpha_1 & \alpha_2 & \dots & \alpha_{n_\beta} \\ 0 & 1 & 0 & \dots & 0 \\ \vdots & \ddots & \ddots & \ddots & \vdots \\ 0 & \dots & 0 & 1 & 0 \end{bmatrix} & \\ \mathbf{0}^{n_\beta\times 2} & & \end{bmatrix} \\
B &= \begin{bmatrix} B_\eta \\ \mathbf{0}^{n_\beta\times 1} \end{bmatrix} \\
C_\eta &= \begin{bmatrix} 0 & -1 \end{bmatrix} \\
C_\beta &= \begin{bmatrix} 1 & \mathbf{0}^{1\times n_\beta - 1} \end{bmatrix} \\
\chi_k &= \begin{bmatrix} x'_{\eta,k} & \beta_k & \Delta\beta_k & \dots & \Delta\beta_{k-n_\beta+1} \end{bmatrix}^\top
\end{aligned} \tag{8}$$

Here w_k is an unknown disturbance input, the main purpose of which is to model the effect of the disturbance δ_k in the incremental beta burst model (7). Therefore we assume w_k to be bounded and i.i.d. with zero mean.

E. State Estimation

Given the estimated parameters θ_β in Section III-C, we propose using a Kalman filter to construct an estimate $\hat{\chi}_k$ of the augmented model state χ_k based on (8). We formulate the Kalman Filter such that the estimated state, $\hat{\chi}_k$ is updated using the latest measurement y_k [18].

We consider the same dynamic model as in (8), with an additional process noise term $\bar{w}_k$ that helps to account for w_k and the error caused by inaccuracies in the models for the nominal beta activity and stimulation response

$$\chi_{k+1} = A(\theta_\beta)\chi_k + Bu_k + \Gamma\bar{w}_k. \tag{9}$$

Here Γ is a diagonal matrix whose elements typically correspond to the covariance of process noise. In the current context Γ can be used to tune the filter to the relative uncertainty affecting the different elements of χ_k. In this case, the third element, which corresponds to the uncertainty on β_k is given a higher value to account for the effect of δ_k.

F. Model Predictive Control

To avoid steady-state errors we design the MPC controller in velocity form, with $\Delta u_k = u_k - u_{k-1}$ as the control variable. We therefore introduce a further augmented nominal model with state χ_k^Δ:

$$\begin{aligned}
\chi_{k+1}^\Delta &= A^\Delta(\theta_\beta)\chi_k^\Delta + B^\Delta\Delta u_k \\
y_k &= C_{Aug}\chi_k^\Delta \\
A^\Delta(\theta_\beta) &= \begin{bmatrix} A(\theta_\beta) & B \\ \mathbf{0}^{1\times n_\chi} & 1 \end{bmatrix} \\
B^\Delta &= \begin{bmatrix} B \\ 1 \end{bmatrix} \\
C_{Aug} &= \begin{bmatrix} C_\eta & C_\beta & 0 \end{bmatrix} \\
\chi_k^\Delta &= \begin{bmatrix} \chi_k \\ u_{k-1} \end{bmatrix}
\end{aligned} \tag{10}$$

The values predicted at time k of the state and control input of (10) at time $k+j$ are denoted $\chi_{j|k}^\Delta$ and $\Delta u_{j|k}$, respectively.

Given the form of the instantaneous cost in (3), we define the following quadratic MPC cost function over an N-step prediction horizon

$$J_{mpc}(\Delta\mathbf{u}, \chi_k^\Delta) = \sum_{j=0}^{N-1} \Big(Q[y_{j|k} - \beta_0]_{\geq 0}^2 + R_\Delta \Delta u_{j|k}^2 + R u_{j|k}^2 \Big). \tag{11}$$

Here Q and R are positive scalar weights and the term $Q[y_{j|k} - \beta_0]_{\geq 0}^2$ ensures that only the predicted values of $y_{j|k} = C_{Aug}\chi_{j|k}^\Delta$ that exceed the reference threshold β_0 are penalized.

We apply the control input $u_k = u_{k-1} + \Delta u_{0|k}^*$, where $\Delta u_{0|k}^*$ is the first element of the optimal sequence $\Delta\mathbf{u}_k = \{\Delta u_{0|k}, \dots, \Delta u_{N-1|k}\}$ for the MPC optimization problem:

$$\Delta\mathbf{u}_k^* = \arg\min_{\Delta\mathbf{u}} J_{mpc}(\Delta\mathbf{u}, \chi_k^\Delta) \tag{12}$$

subject to the augmented nominal model dynamics (10) with $\chi_{k+j} = \chi_{j|k}$ and $\Delta u_{k+j} = \Delta u_{j|k}$, and subject to the input constraints $u_{j|k} \in [0, u_{\max}]$, for all $j = 0, \dots, N-1$.

IV. Numerical Examples

This section describes simulations in which the performance of the model predictive control law defined in Section III is compared with that of a bang-bang controller and a PI controller. In Section IV-A we discuss the identification of an ARX model representing the dynamics of beta-band activity. Then, in Section IV-B, we compare the closed loop performance of the three controllers. To represent the variability in the response of different patients, these closed loop simulations were run multiple times with the same trajectory for the nominal beta activity, but with the initial parameters for the stimulation response model (2) disturbed from their nominal values after discretization by up to 30%.

The first set of closed loop tests in Section IV-B use a simulated nominal beta activity pattern with various levels of power in the injected measurement noise ζ. This makes it possible to compare the robustness of the controllers to varying levels of noise. The second set of tests use the beta activity extracted via *in vivo* recordings from a Parkinsonian patient to provide more realistic test conditions.

A. Linear Nominal Activity Model Identification

A linear model for the nominal beta activity was identified as described in Sections III-B and III-C using beta activity from *in vivo* recordings from a Parkinsonian patient. The sampling interval was $T_s = 0.02\,\text{s}$. Figure 1 shows the one-step-ahead prediction accuracy of the estimated model after a 5 second identification period, with model order $n_\beta = 5$. Here the estimated signal $\hat{\beta}_k$ is obtained by adding $\Delta\beta_k$ generated by the model (7) to the signal $y_{k-1} = \ln\big(z((k-1)T_s)\big)$ observed at the previous time step. Figure 2 shows the mean-square one-step-ahead prediction error of the model (7) when the parameter identification is performed with varying levels of noise power.

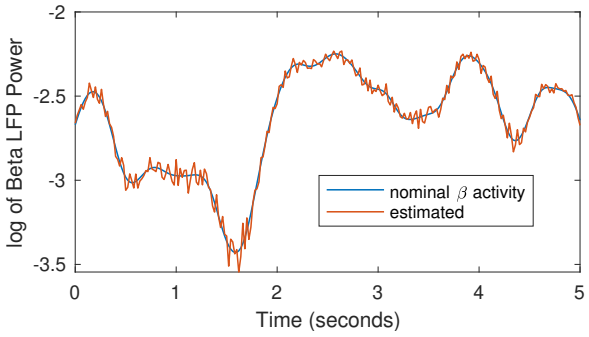

Fig. 1: Comparison of actual and estimated nominal beta activity. The blue plot shows $y_k = \ln\big(z(kT_s)\big)$, where $z(t)$ is the LFP signal observed *in vivo* with no stimulation ($\eta(t) = 0$). The red plot shows the one-step-ahead estimate $\hat{\beta}_k = y_{k-1} + \Delta\beta_k$, where $\Delta\beta_k$ is the output of the model (7).

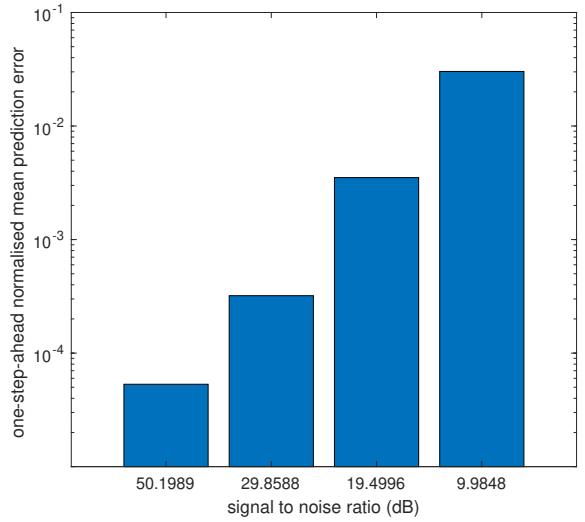

Fig. 2: Beta activity estimation error after identification of the parameters of the model (7) at various noise levels.

B. Comparison with bang-bang and PI Controllers

The bang-bang controller, $u_{\mathrm{BB},k}$, provides a constant level of stimulation whenever the measured beta activity exceeds some threshold, and zero stimulation otherwise:

$$u_{\mathrm{BB},k} = \begin{cases} u_{max} & \text{if } y_k > y_{\mathbb{BB},threshold} \\ 0 & \text{otherwise} \end{cases} \tag{13}$$

The PI controller is implemented in difference form: $u_{\mathrm{PI},k} = u_{\mathrm{PI},k-1} + \Delta u_{\mathrm{PI},k}$ using the error signal $e_k = z(kT_s) - z_0$:

$$\Delta u_{\mathrm{PI},k} = \; K_P \Delta e_k + K_I T_s e_k \tag{14}$$

Simulations were run with various levels of perturbation applied to the parameters of the stimulation response model, with parameters perturbed according to a uniform distribution at the beginning of each simulation run. Only parameter perturbations resulting in an open-loop stable model and causing a change in static gain of no more than 30% relative to the nominal model were considered.

The same nominal beta trajectory was used test MPC, bang-bang and PI controllers. The nominal stimulation response model was used to tune the bang-bang and PI controllers, as well as to define the MPC prediction model. The performance metrics used for comparison are the normalized difference in mean squared positive error $\bar{e}$ and normalized difference in total control input $\bar{u}$.

$$\bar{e}_{\{\mathrm{BB,PI}\}} = \frac{\sum_{j=0}^{N_{\mathrm{sim}}} \left(\left[y_{j,\{\mathrm{BB,PI}\}} - \beta_0 \right]_{>0} - \left[y_{j,\mathrm{MPC}} - \beta_0 \right]_{>0} \right)}{\sum_{j=0}^{N_{\mathrm{sim}}} \left[y_{j,\mathrm{MPC}} - \beta_0 \right]_{>0}} \tag{15}$$

$$\bar{u}_{\{BB,PI\}} = \frac{\sum_{j=0}^{N_{\mathrm{sim}}} \left(u_{j,\{\mathrm{BB,PI}\}} - u_{j,\mathrm{MPC}} \right)}{\sum_{j=0}^{N_{\mathrm{sim}}} u_{j,\mathrm{MPC}}}. \tag{16}$$

Therefore, positive values for these metrics indicate better performance achieved by MPC than the alternative controller.

1) Simulated Beta Activity: Simulations were run at a sampling rate of 50Hz, for a duration of 20 seconds. The nominal β estimation period was set to 5 seconds and signal to noise ratios of 50, 30, 20 and 10 dB were used to define the measurement noise ζ in (1) and the process noise w in (8). For each noise level, 50 simulations were performed. We compare the performance of bang-bang and PID control with that of MPC in Fig. 3. The trajectories show that MPC reaches steady state faster and with fewer oscillations than the PI controller, while bang-bang suppresses activity below the threshold due to noise-induced triggering of the maximum input.

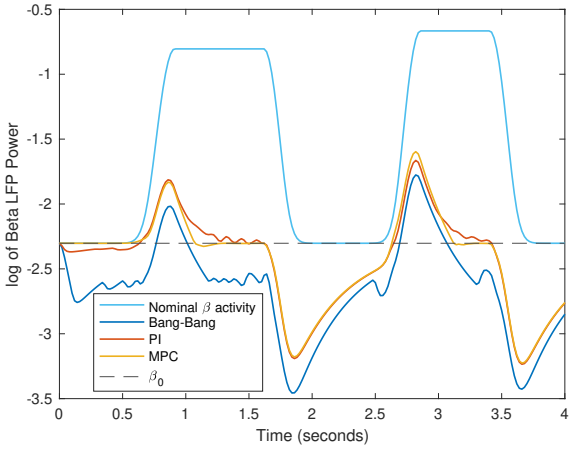

Fig. 3: Beta response for MPC, bang-bang and PI controllers with 30% parameter disturbance, 12dB signal to noise ratio, and nominal beta activity defined by a simulation model.

Figure 5 shows that MPC results in significant reduction in tracking error and total stimulation compared to bang-bang controller across all noise and initial parameter error conditions. When compared with PI, MPC shows a reduction in required control input except at the lowest tested noise condition, and a consistent reduction in error across all test conditions.

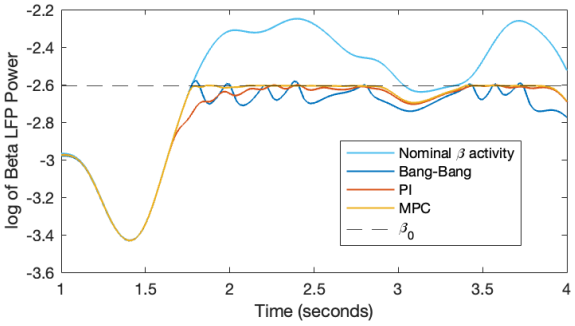

Fig. 4: Beta response for MPC, bang-bang and PI controllers with 30% parameter disturbance and with nominal beta activity defined using patient data.

2) Patient Data: The performance of the controllers was also compared using beta power extracted from 220 seconds of data taken from a Parkinsonian patient recorded from an implanted DBS electrode with stimulation turned off as the nominal beta activity. Again, the nominal beta activity estimation period was 5 seconds, and the stimulation effect model parameters were perturbed by varying amounts. All controllers used the same tuning as for the simulated runs, and the threshold level was set as the 75th percentile of the measured beta LFP power.

The comparison of MPC and bang-bang control trajectories in Fig. 4 show that again, MPC shows smoother steady state behaviour around the reference. Fig. 6 shows a significant improvement in both control input and tracking error across a range of parameter error values. The comparison with PI control shows consistently lower control input, but a greater error for MPC for parameter errors of 20% and higher. For greater parameter errors, the increase in error remains on average lower than the reduction in control input, which exceeds 25%. These results indicate that the performance benefits of MPC are smaller at higher levels of modelling error. In addition, the performance of the PI controller was more robust to variations in the threshold β_0. The trajectories for the various controllers are shown in Fig. 5. The MPC controller results in smoother tracking of the reference, and lower oscillations around the steady state behaviour. The trajectories for the Bang-Bang and PI controllers show greater oscillations around steady state, indicating the advantage of predicting the beta activity.

V. Concluding Remarks and Further Work

The simulation results presented in this paper show that MPC provides improvements over bang-bang and PI controllers in terms of both energy efficiency and error tracking for up to 20% error in model parameters. These results warrant further investigation of the use of model predictive control in this context, including testing in patients. We note that large initial parameter errors have a significant impact on the performance of MPC, suggesting the need to investigate adaptive control strategies which can recursively update the stimulation response model parameters to fit each patient, as well as robust controllers that can account for model uncertainty characterised in terms of bounds on parameters and external disturbances.

References

[1] C. Sarica, C. Conner, K. Yamamoto, A. Yang, J. Germann, M. Lannon, and et al., "Trends and disparities in deep brain stimulation utilization in the united states: a nationwide inpatient sample analysis from 1993 to 2017," *Lancet Regional Health. Americas*, p. 100599, 2023.

[2] S. J. Schiff, "Towards model-based control of parkinson's disease," *Phil. Trans. R. Soc. A*, vol. 368, pp. 2269–2308, 2010.

[3] J. Fleming, E. Dunn, and M. Lowery, "Simulation of closed-loop deep brain stimulation control schemes for suppression of pathological beta oscillations in parkinson's disease," *Front. Neurosci.*, vol. 14, no. 166, 2020.

[4] P. Silberstein, A. Oliviero, V. Di Lazzaro, A. Insola, P. Mazzone, and P. Brown, "Oscillatory pallidal local field potential activity inversely correlates with limb dyskinesias in parkinson's disease," *Exp. Neurol.*, vol. 194, pp. 523–529, 2005.

[5] G. Tinkhauser, F. Torrecillos, A. Pogosyan, A. Mostofi, M. Bange, P. Fischer, and et al., "The cumulative effect of transient synchrony states on motor performance in Parkinson's disease," *J. Neurosci.*, vol. 40, pp. 1571–1580, 2020.

[6] S. Little, A. Pogosyan, S. Neal, B. Zavala, L. Zrinzo, M. Hariz, and et al., "Adaptive deep brain stimulation in advanced parkinson disease," *Ann. Neurol.*, vol. 74, pp. 449–457, 2013.

[7] M. Arlotti, S. Marceglia, G. Foffani, J. Volkmann, A. M. Lozano, E. Moro, and et al., "Eight-hours adaptive deep brain stimulation in patients with parkinson disease," *Neurology*, vol. 90, pp. e971–e976, 2018.

[8] A. Velisar, J. Syrkin-Nikolau, Z. Blumenfeld, M. Trager, M. F. Afzal, V. Prabhakar, and H. Bronte-Stewart, "Dual threshold neural closed loop deep brain stimulation in parkinson disease patients," *Brain Stimulation*, vol. 12, pp. 868–876, 2019.

[9] M. Petrucci, R. Anderson, J. O'Day, K. Y.M., J. A. Herron, and H. Bronte-Stewart, "A closed-loop deep brain stimulation approach for mitigating burst durations in people with parkinson's disease.," in *Annual International Conference of the IEEE Engineering in Medicine and Biology Society.*, pp. 3617–3620, 2020.

[10] J. Fleming, S. Senneff, and M. Lowery, "Multivariable closed-loop control of deep brain stimulation for parkinson's disease," *Journal of Neural Engineering*, vol. 20, p. 056029, 2023.

[11] F. Su, J. Wang, S. Niu, H. Li, B. Deng, C. Liu, and X. Wei, "Nonlinear predictive control for adaptive adjustments of deep brain stimulation parameters in basal ganglia–thalamic network," *Neural Networks*, vol. 98, pp. 283–295, 2018.

[12] A. Haddock, A. Velisar, J. Herron, H. Bronte-Stewart, and H. Chizeck, "Model predictive control of deep brain stimulation for parkinsonian tremor," in *8th International IEEE EMBS Conference on Neural Engineering*, (Shanghai, China), pp. 358–362, 2017.

[13] M. Ahmadipour, M. Barkhordari-Yazdi, and S. Seydnejad, "Subspace-based predictive control of parkinson's disease: A model-based study," *Neural Networks*, vol. 142, pp. 680–689, 2021.

[14] J. Debarros, S. He, G. Tinkhauser, J. Fleming, T. Denison, M. Cannon, P. Brown, and H. Tan, "Modelling LFP response to electrical stimulation in parkinson's disease (PD): a theoretical and practical framework." unpublished.

[15] E. M. Moraud, G. Tinkhauser, M. Agrawal, P. Brown, and R. Bogacz, "Predicting beta bursts from local field potentials to improve closed-loop dbs paradigms in parkinson's patients," in *2018 40th Annual International Conference of the IEEE Engineering in Medicine and Biology Society (EMBC)*, pp. 3766–3796, 2018.

[16] B. Abdi-Sargezeh, S. Shirani, A. Sharma, P. A. Starr, S. Little, and A. Oswal, "Predicting long and short duration beta bursts from sub-thalamic nucleus local field potential activity in parkinson's disease," *bioRxiv*, 2023.

[17] J. Frey, J. Cagle, K. Johnson, J. Wong, H. J.D, C. Butson, and et al., "Past, present, and future of deep brain stimulation: Hardware, software, imaging, physiology and novel approaches," *Frontiers in neurology*, vol. 13, p. 825178, 2022.

[18] G. Franklin, P. J. D., and M. L. Workman, *Digital Control of Dynamic Systems*. Half Moon Bay: Ellis-Kagle Press, 3. ed., 1998.

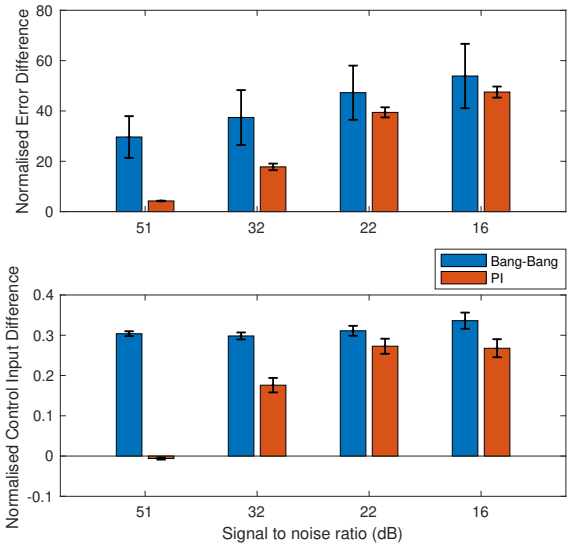

(a) 10% parameter error

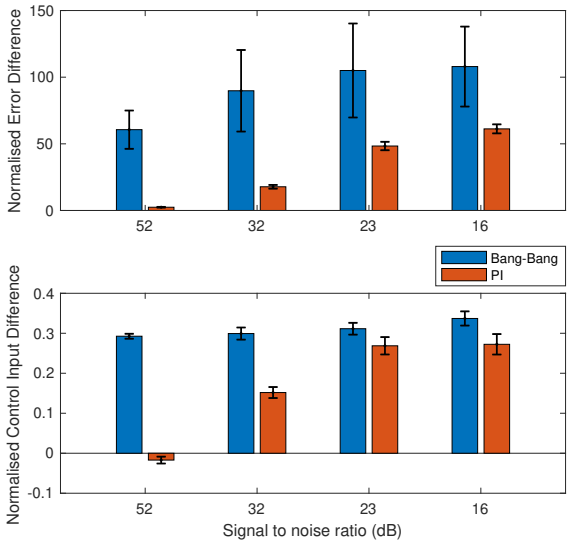

(b) 30% parameter error

Fig. 5: Differences in error and control input between MPC and bang-bang (blue, $e_{\text{total},\{\text{BB}\}}$ and $u_{\text{total},\{\text{BB}\}}$) and between MPC and PI (orange, $e_{\text{total},\{\text{PI}\}}$ and $u_{\text{total},\{\text{PI}\}}$), for various levels of measurement noise ζ in the envelope of beta-band activity, with nominal beta activity defined by a simulation model (positive values indicate better MPC performance).

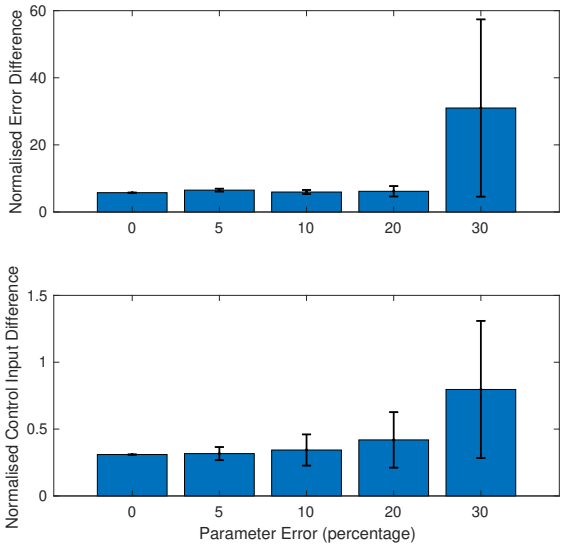

(a) Bang-bang

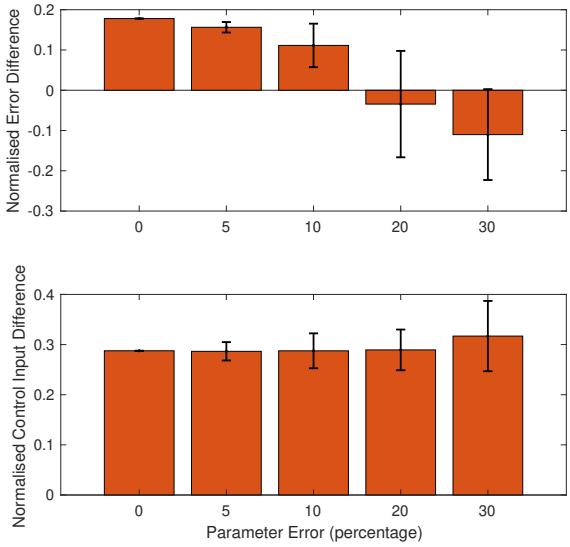

(b) PI

Fig. 6: Differences in error and control input between MPC and bang-bang (blue, $e_{\text{total},\{\text{BB}\}}$ and $u_{\text{total},\{\text{BB}\}}$) and between MPC and PI (orange, $e_{\text{total},\{\text{PI}\}}$ and $u_{\text{total},\{\text{PI}\}}$), for various levels of initial error in parameters of the stimulation response model with nominal beta activity defined using patient data (positive values indicate better MPC performance).